Coupled Systems Mechanics, *Vol. 7, No. 6 (2018) 649-668*
DOI: https://doi.org/10.12989/csm.2018.7.6.649

Fluid-structure interaction system predicting both internal pore pressure and outside hydrodynamic pressure

Emina Hadzalic[*1,3], Adnan Ibrahimbegovic[1,2a] and Samir Dolarevic[3b]

[1]*Université de Technologie de Compiègne, Laboratoire Roberval de Mécanique, Centre de Recherche Royallieu, 60200 Compiègne, France*
[2]*Institut Universitaire de France*
[3]*Faculty of Civil Engineering, University of Sarajevo, Patriotske lige 30, Sarajevo 71000, Bosnia and Herzegovina*

(Received June 5, 2018, Revised August 26, 2018, Accepted August 27, 2018)

Abstract. In this paper, we present a numerical model for fluid-structure interaction between structure built of porous media and acoustic fluid, which provides both pore pressure inside porous media and hydrodynamic pressures and hydrodynamic forces exerted on the upstream face of the structure in an unified manner and simplifies fluid-structure interaction problems. The first original feature of the proposed model concerns the structure built of saturated porous medium whose response is obtained with coupled discrete beam lattice model, which is based on Voronoi cell representation with cohesive links as linear elastic Timoshenko beam finite elements. The motion of the pore fluid is governed by Darcy's law, and the coupling between the solid phase and the pore fluid is introduced in the model through Biot's porous media theory. The pore pressure field is discretized with CST (Constant Strain Triangle) finite elements, which coincide with Delaunay triangles. By exploiting Hammer quadrature rule for numerical integration on CST elements, and duality property between Voronoi diagram and Delaunay triangulation, the numerical implementation of the coupling results with an additional pore pressure degree of freedom placed at each node of a Timoshenko beam finite element. The second original point of the model concerns the motion of the outside fluid which is modeled with mixed displacement/pressure based formulation. The chosen finite element representations of the structure response and the outside fluid motion ensures for the structure and fluid finite elements to be connected directly at the common nodes at the fluid-structure interface, because they share both the displacement and the pressure degrees of freedom. Numerical simulations presented in this paper show an excellent agreement between the numerically obtained results and the analytical solutions.

Keywords: acoustic fluid-structure interaction; dam-reservoir system; coupled discrete beam lattice model; saturated porous media; mixed displacement/pressure based formulation; hydrodynamic pressure

*Corresponding author, Corresponding author, Ph.D. student,
E-mail: emina.hadzalic@utc.fr or emina.hadzalic@gf.unsa.ba
[a]Chair for Computational Mechanics, Professor, E-mail: adnan.ibrahimbegovic@utc.fr
[b]Professor, E-mail: samir.dolarevic@gf.unsa.ba

http://www.techno-press.org/?journal=csm&subpage=8 ISSN: 2234-2184 (Print), 2234-2192 (Online)

1. Introduction

When the fluid-structure systems such as dam-reservoir are subjected to dynamic loading, next to the hydrostatic pressures, additional hydrodynamic pressures are exerted on the upstream face of the structure. In order to conduct the sound design of the structure, the value and the distribution of hydrodynamic pressure have to be computed either from analytical solutions proposed in the literature or with numerical methods. In everyday engineering practice the analytical solutions or numerical models that tend to have wider application are usually the ones that are predictive, and yet simple enough.

The problem of evaluating the value and the distribution of the hydrodynamic pressure was first examined in the work of Westergaard (Westergaard 1933). Westergaard proposed an analytical solution for a rigid dam with vertical upstream face subjected to horizontal harmonic motion. Von Kármán proposed an analytical solution, which is very close to the Westergaard's using linear momentum balance principle (Von Kármán 1933). Later, Chwang and Housner, also using momentum method, derived the analytical solution for the general case of an inclined upstream face of the dam subjected to constant horizontal acceleration (Chwang and Housner 1978). In the second part of his work, Chwang derived the analytical solution using two-dimensional potential flow theory (Chwang 1978). The computation of hydrodynamic pressure distribution exerted on the retaining structures due to submerged backfill soils is in close relation with computation of hydrodynamic pressure distribution exerted on the upstream face of the dams. For example, Matsuzawa *et al.* (Matsuzawa *et al.* 1985) provided generalized apparent angle of seismic coefficient to compute hydrodynamic pressure distribution on retaining structures, depending on the soil permeability, inclined wall angle and ratio of the backfill length to height.

In the category of fluid-structure interaction problems in which fall the structures such as dam-reservoir systems, storage tanks or water containers, the outside fluid motion can be regarded as small. This allows for the outside fluid to be modeled as Lagrangian, and the governing equations to be derived from acoustic wave theory. For evaluating the values and distribution of hydrodynamic pressure exerted on the upstream face of the dam, many numerical models of acoustic fluid-structure interaction have been proposed. Here, the structure is usually regarded as rigid or linear elastic and the response of the structure is obtained with continuum type of models in which the domain is discretized with 2D or 3D finite elements, which have displacement degrees of freedom per node. The numerical models of acoustic fluid-structure interaction in which the outside fluid motion is described with pressure based formulation can be found in (Zienkiewicz and Bettess 1978, Mitra and Sinhamahapatra 2008, Keivani *et al.* 2013, Mandal and Maity 2015). In the pressure based formulation, only unknown degree of freedom per node of a fluid element is the pressure. Hence, a special treatment of the fluid-structure interface is needed because the structure and the fluid finite element do not share the same degrees of freedom. In (Hamdi *et al.* 1978, Chen and Taylor 1990, Pelecanos *et al.* 2013) the fluid motion is described with displacement based finite element formulation. The advantage of this formulation is that both the fluid and structure share the same displacement degrees of freedom. However, one has to keep in mind that in fluid-structure interaction problems, the outside fluid acts as a source of the saturation keeping the material of the structure fully saturated at each time step. Hence, we need to take into account the presence of the pore fluid on the response of the structure which is very important, for example in the case of earth dams where an increase in the pore pressure in dynamic setting can lead to the liquefaction phenomenon. In other words, we ought to model the structure as a saturated porous medium. In (Wang and Wang 2007), the structure is modeled as a saturated

porous medium and the motion of the outside fluid is described with potential based finite element formulation. Here, special numerical treatment of the fluid-structure interfaces is also required.

In this paper, we present a numerical model of acoustic fluid-structure interaction for dynamic loading. Here, we focus on the capabilities of the proposed model for predicting hydrodynamic pressure and hydrodynamic forces exerted on the upstream face of the structure. Furthermore, we aim to provide a numerical model, which is predictive, simple and comprehensive enough to be accepted as an everyday tool in structural analysis. Thus, we assume that the behavior of the structure is governed by Hooke's linear elastic law. We consider the structure as saturated porous medium whose response is obtained with coupled discrete beam lattice model. The discrete beam lattice model of the structure is based on the Voronoi cell representation in which the cohesive links are modeled with linear elastic Timoshenko beam finite elements. The coupling between the solid phase and the pore fluid in the model is enforced through Biot's porous media theory. For describing the motion of the outside fluid, we choose the mixed displacement/pressure based formulation (Bathe *et al.* 1995, Wang and Bathe 1997). In this formulation, the unknown is both displacement and pressure fields. Now, having the structure represented as a saturated porous medium in a combination with the mixed formulation for the outside fluid, we are able to directly connect the outside fluid and structure finite elements at the common nodes because they share both displacement and pressure degrees of freedom. With this unified approach, we eliminate any need for special numerical treatment of the fluid-structure interface and computations of all unknown fields can be performed in a fully monolithic manner.

The outline of the paper is as follows: In Section 2, we provide a short overview of the fundamental analytical solutions for hydrodynamic pressure distribution. In Section 3, we provide a brief description and finite element formulation of the structure response and the outside fluid motion. In Section 4, we present the results of several numerical simulations. In section 5, we give our concluding remarks.

2. Analytical solutions

Westergaard's solution. Westergaard is the first who studied the problem of evaluating the hydrodynamic pressures exerted on the upstream face of the dam. His work was focused on the simple two-dimensional dam-reservoir system subjected to the horizontal harmonic ground motion (Fig. 1). The dam was assumed to be rigid with vertical upstream face, and the length of the reservoir was assumed to be infinite. Westergaard derived an analytical solution for the hydrodynamic pressure distribution in terms of series of sine functions. Maximum hydrodynamic pressure distribution on the vertical upstream face of the rigid dam, according to Westergaard, is described with following expression

$$p = \frac{8a_0\rho H}{\pi^2} \sum_{1,3,5\ldots}^{n} \frac{1}{n^2 c_n} \sin\left(\frac{n\pi y}{2H}\right) \tag{1}$$

$$c_n = \sqrt{1 - \frac{16\rho H^2}{n^2 gKT^2}} \tag{2}$$

where a_0 is the maximum horizontal acceleration of the foundation, ρ is the density of the retained water, H is the depth of the reservoir, K is the bulk modulus of water, and T is the period of the

horizontal acceleration of the foundation.

Based on the previous solution, Westergaard proposed a simpler expression which results in a parabolic distribution of hydrodynamic pressure

$$p = 0.875 a_0 \rho \sqrt{Hy} \tag{3}$$

This expression, even though represents a conservative approximation, gives satisfactory results and is widely used in everyday engineering practice.

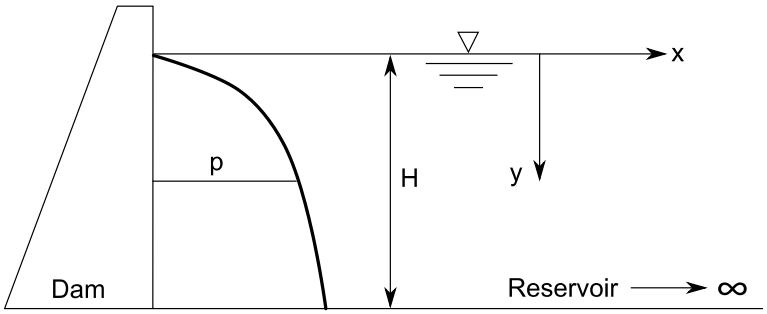

Fig. 1 Dam-reservoir system studied by Westergaard (Westergaard 1933)

According to Westergaard, total horizontal force exerted on the vertical, upstream face of the dam is equal to

$$F = F_x = 0.543 a_0 \rho H^2 \tag{4}$$

Von Kármán's solution. An analytical solution very close to Westergaard's was derived by von Kármán. In his work, von Kármán exploited linear momentum-balance principle and derived an expression for hydrodynamic pressure distribution which reads as

$$p = 0.707 a_0 \rho \sqrt{Hy} \tag{5}$$

According to von Kármán, total horizontal force exerted on the vertical, upstream face of the dam is equal to

$$F = F_x = 0.555 a_0 \rho H^2 \tag{6}$$

Chwang's solution. For a general case of a rigid dam with an inclined upstream face with a constant slope subjected to uniform horizontal acceleration a_0 (Fig. 2), Chwang and Housner derived analytical solution using the momentum balance method proposed by von Kármán. The fluid in the reservoir is assumed to be incompressible and inviscid.

In their analytical solution, as in the Westergaard's and von Kármán's solutions, the value of hydrodynamic pressures ranges from zero at the top of the reservoir to maximum at the bottom of the reservoir. Chwang, in the second part of his work, derived an analytical solution for hydrodynamic pressure distribution using two-dimensional potential flow theory. Here, except for the case of vertical upstream face, the maximum value of hydrodynamic pressure does not occur at the bottom of the reservoir but is moved up to a certain distance.

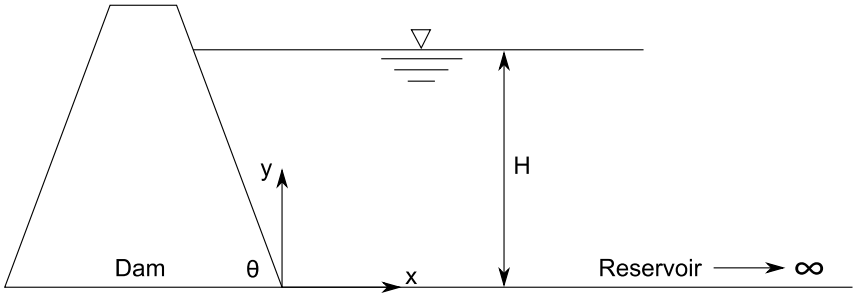

Fig. 2 Dam-reservoir system studied by (Chwang and Housner 1978) and (Chwang 1978)

The hydrodynamic pressure distribution on the inclined upstream face is described with following expression

$$p = C_p a_0 \rho H \tag{7}$$

where C_p is the pressure coefficient. Total horizontal and vertical force exerted on the inclined upstream face of the dam are equal to

$$F_x = C_x a_0 \rho H^2 \tag{8}$$

$$F_y = C_y a_0 \rho H^2 \tag{9}$$

where C_x and C_y are force coefficients. The expressions for computing the values of pressure and force coefficients can be found in (Chwang and Housner 1978) and (Chwang 1978).

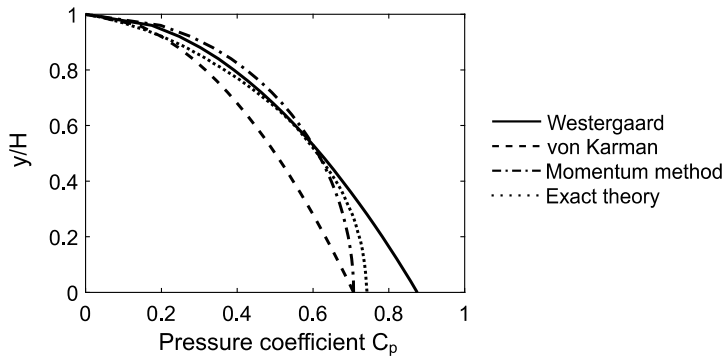

Fig. 3 Comparison of analytical solutions for vertical upstream face ($\theta = 90°$)

For the case of the vertical upstream face, the exact method gives the value of force coefficient $C_x = 0.543$ which is the same as Westergaard's solution, and the momentum method gives the value $C_x = 0.555$ which is the same as von Kármán's solution. The comparison between the analytical solutions for hydrodynamic pressure distribution on the vertical upstream face of the dam is shown in Fig. 3.

3. Numerical model of acoustic fluid-structure interaction

3.1 Structure built of saturated porous media

For the numerical representation of the structure response we use a discrete lattice model based on the Voronoi cell representation of the domain. The advantage of discrete lattice models based on the Voronoi cell discretization is that they are able to reproduce the linear elastic part of the response of an equivalent continuum model (Ibrahimbegovic and Delaplace 2003). Namely, the main idea is to represent the structure as an assembly of Voronoi cells, where each two Voronoi cells are held together by cohesive links. We model the behavior of these cohesive links with finite elements. Thus, the macro-scale response of the structure is obtained on the mesh of 1D finite elements. The discrete model with truss bar elements with embedded strong discontinuity in axial direction (Benkemoun *et al.* 2010, Benkemoun *et al.* 2012), or with Timsohenko beam finite elements with embedded strong discontinuities in both axial and transverse direction have been successfully used in predicting the response of heterogeneous materials such as the soils, rocks and concrete (Nikolic *et al.* 2015, Nikolic and Ibrahimbegovic 2015, Hadzalic *et al.* 2018), both in 2D and 3D setting.

Here, our goal is to numerically determine the values of hydrodynamic pressure exerted on the upstream face of the structure, and to compare the results against analytical solutions with the aim to validate the numerical model of acoustic fluid-structure interaction for everyday use in structural analysis. Thus, for cohesive links we choose linear elastic Timoshenko beam finite elements. The mesh and cross sectional properties of Timoshenko beam finite elements are obtained from Delaunay triangulation and Voronoi diagram (Fig. 4). The end result of Delaunay triangulation performed on a certain domain is a mesh of triangles. We place a cohesive link along every edge of triangle. This is made possible by exploiting the duality property between Delaunay triangulation and Voronoi diagram. This property implies that every cohesive link connects the centers of two adjacent Voronoi cells, and that each cohesive link is perpendicular to the edge shared between two adjacent cells. Thus, the height of the cross section of the finite element, which model the behavior of the cohesive link, is equal to the length of the shared edge.

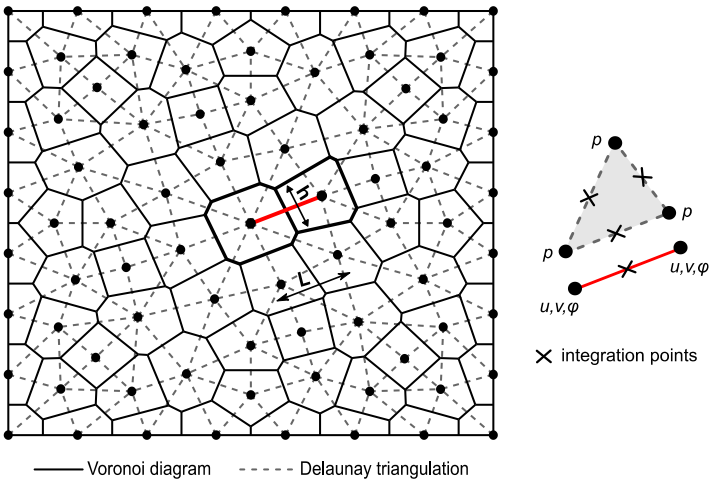

Fig. 4 Voronoi diagram and Delaunay triangulation

To take into account the influence of the pore fluid, Biot's porous media theory is introduced in the model. We assume that the pore fluid flow is spread across the mesh of CST finite elements, which coincide with triangles obtained with Delaunay triangulation. By exploiting Hammer quadrature rule for numerical integration on CST elements (Zienkiewicz and Taylor 2005), which positions each integration point at the center of each edge of triangle, and duality property between the Voronoi cell and Delaunay triangle representations, we are able to simplify the problem of the numerical implementation of the coupling. Namely, the positions of the integration points for triangular finite elements coincide with the positions of integration points for Timoshenko beam finite elements (Fig. 4). Note that for Timoshenko beam finite element we choose only one Gauss integration point located at the center of the beam, and that center of each beam is located at the edge shared between two adjacent Voronoi cells. Thus, we can treat the pore pressure as an additional degree of freedom placed at each node of Timoshenko beam finite element, and assume that the coupling between the mechanics and the pore fluid flow occurs through axial direction of Timoshenko beam finite element, (Nikolic *et al.* 2016, Hadzalic *et al.* 2018).

3.1.1 Finite element formulation of the coupled problem in dynamic setting

The problem of interaction of the solid phase and the pore fluid in Biot's porous media theory (Biot 1941) is described with equilibrium and continuity equations. Here, we refer to the equation of motion instead of equilibrium equation. In the formulation of the coupled problem, Biot's theory exploits Terzaghi's principle of effective stresses that states that the total normal stress is equal to the sum of effective stress σ' and pore pressure p

$$\sigma = \sigma' - bp \tag{10}$$

where b is Biot's coefficient. Here, σ' is assumed to be positive in tension, and p positive in compression.

This principle is exploited in the formulation of the equation of motions for Timoshenko beam. The strong form of equations of motion is derived based on the d'Alambert principle (Ibrahimbegovic 2009) and is written as

$$-\rho A\frac{\partial^2 u}{\partial t^2}+\frac{\partial N}{\partial x}+n(x,t)=0 \tag{11}$$

$$-\rho A\frac{\partial^2 v}{\partial t^2}+\frac{\partial V}{\partial x}+q(x,t)=0 \tag{12}$$

$$-\rho I\frac{\partial^2 \theta}{\partial t^2}+\frac{\partial M}{\partial x}+V+m(x,t)=0 \tag{13}$$

where ρ is the mass density, A is the area of the cross section of the Timoshenko beam, I is the second moment of inertia of the cross section, $\mathbf{u}=[u, v, \theta]$ is the displacement vector, $\mathbf{F}=[N, V, M]$ $=[N'\text{-}bpA, V', M']$ is the internal force vector, and $\mathbf{f}=[n, q, m]$ is the vector of distributed loads.

The pore fluid flow in the coupled discrete model is spread across the mesh of CST finite elements, and is governed by Darcy's law. The coupling between the mechanics and pore fluid flow occurs in axial direction of Timoshenko beam finite elements. The continuity equation for pore fluid flow is written as

$$\frac{1}{M}\dot{p}+b(\nabla\cdot\dot{u})-\frac{k}{\gamma_f}\nabla\cdot(\nabla p)=0 \tag{14}$$

where p is the pore pressure, M is Biot's modulus, k is the coefficient of permeability of isotropic porous medium, and γ_f is the specific weight of the fluid.

Following the standard finite element discretization procedure and introducing finite elements approximations we obtain following system of equations governing the discrete problem, for a typical finite element written as

$$\begin{aligned} \mathbf{M}^e\ddot{\bar{\mathbf{u}}} + \mathbf{K}^e\bar{\mathbf{u}} - \mathbf{Q}^e\bar{\mathbf{p}}' &= \mathbf{f}^{e,ext} \\ \mathbf{Q}^{e,T}\dot{\bar{\mathbf{u}}} + \mathbf{S}^e\dot{\bar{\mathbf{p}}}' + \mathbf{H}^e\bar{\mathbf{p}}' &= \mathbf{q}^{e,ext} \end{aligned} \tag{15}$$

where $\bar{\mathbf{u}}$ is the vector of unknown nodal displacements, $\bar{\mathbf{p}}$ is the vector of unknown nodal pore pressures, $\mathbf{f}^{e.ext}$ and $\mathbf{q}^{e,ext}$ are the external load vectors, $\mathbf{M}^e$ is the mass matrix, $\mathbf{K}^e$ is the stiffness matrix, $\mathbf{Q}^e$ is the coupling matrix, $\mathbf{S}^e$ is the compressibility matrix, and $\mathbf{H}^e$ is the permeability matrix given as

$$\begin{aligned} &\mathbf{M}^e = \int_0^{L^e} \mathbf{N}_u^{s,T}\,\mathbf{C}^m\,\mathbf{N}_u^s\,dx,\ \mathbf{K}^e = \int_0^{L^e} \mathbf{B}_u^{s,T}\,\mathbf{C}^k\,\mathbf{B}_u^s\,dx \\ &\mathbf{Q}^e = \int_0^{L^e} \mathbf{B}_{up}^{s,T} b\,\mathbf{N}_{up}^s\,dx, \qquad \mathbf{S}^e = \int_{\Omega_{CST}^e} \mathbf{N}_p^{s,T}\frac{1}{M}\mathbf{N}_p^s\,d\Omega,\ \ \mathbf{H}^e = \int_{\Omega_{CST}^e} \left(\nabla\mathbf{N}_p^s\right)^T\frac{k}{\gamma_f}\mathbf{B}_p^s\,d\Omega \\ &\mathbf{C}^m = \begin{bmatrix} \rho A^e & 0 & 0 \\ 0 & \rho A^e & 0 \\ 0 & 0 & \rho I^e \end{bmatrix},\ \mathbf{C}^k = \begin{bmatrix} EA^e & 0 & 0 \\ 0 & k_s GA^e & 0 \\ 0 & 0 & EI^e \end{bmatrix} \\ &\mathbf{N}_{up}^s = \left\{N_1, N_2\right\},\ \ \mathbf{B}_{up}^s = \begin{bmatrix} B_1 & 0 & 0 & B_2 & 0 & 0 \end{bmatrix} \end{aligned} \tag{16}$$

where E is Young's modulus, $G=E/2(1+\nu)$ is the shear modulus with ν as Poisson's ratio, and k_s is the shear correction factor.

The Timoshenko beam finite element has two nodes, and three degrees of freedom per node: axial displacement, transverse displacement and rotation of cross section. The displacement fields are interpolated with standard, linear interpolation functions. The pore pressure field is approximated with CST finite elements

$$\mathbf{u} = \mathbf{N}_u^s\bar{\mathbf{u}},\ \ p = \mathbf{N}_p^s\bar{\mathrm{p}} \tag{17}$$

where

$$\mathbf{u}^T = \left\{u, v, \theta\right\},\ \bar{\mathbf{u}}^T = \left\{u_1, v_1, \theta_1, u_2, v_2, \theta_2\right\},\ \bar{\mathbf{p}}^T = \left\{p_1, p_2, p_3\right\},\ \bar{\mathbf{p}}'^T = \left\{p_1, p_2\right\} \tag{18}$$

$$\begin{aligned} &\mathbf{N}_u^s = \begin{bmatrix} N_1 & 0 & 0 & N_2 & 0 & 0 \\ 0 & N_1 & 0 & 0 & N_2 & 0 \\ 0 & 0 & N_1 & 0 & 0 & N_2 \end{bmatrix},\ \left\{N_1, N_2\right\} = \left\{1 - \frac{x}{L^e}, \frac{x}{L^e}\right\} \\ &\mathbf{N}_p^s = \left\{N_1^p, N_2^p, N_3^p\right\},\ N_1^p = \frac{1}{2A}\left[\left(x_2y_3 - x_3y_2\right) + \left(y_2 - y_3\right)x + \left(x_3 - x_2\right)y\right] \\ &N_2^p = \frac{1}{2A}\left[\left(x_3y_1 - x_1y_3\right) + \left(y_3 - y_1\right)x + \left(x_1 - x_3\right)y\right] \\ &N_3^p = \frac{1}{2A}\left[\left(x_1y_2 - x_2y_1\right) + \left(y_1 - y_2\right)x + \left(x_2 - x_1\right)y\right] \end{aligned} \tag{19}$$

Here, A is the area of CST element, x, y are global coordinates and x_i, y_i are nodal coordinates of CST element. For simplicity, we assume that Timoshenko beam finite element is placed along global x axis, which can be easily generalized by using local element frame.

The strain fields for standard Timoshenko beam finite element, and pore pressure gradient are written as

$$\boldsymbol{\varepsilon} = \mathbf{B}_u^s \bar{\mathbf{u}}, \ \nabla p = \nabla \mathbf{N}_p^s \bar{\mathrm{p}} \tag{20}$$

where

$$\boldsymbol{\varepsilon}^T = \{\varepsilon, \gamma, \kappa\}, \ \mathbf{B}_u^s = \begin{bmatrix} B_1 & 0 & 0 & B_2 & 0 & 0 \\ 0 & B_1 & -N_1 & 0 & B_2 & -N_2 \\ 0 & 0 & B_1 & 0 & 0 & B_2 \end{bmatrix} \tag{21}$$

The time discretizations of the displacement and pore pressure fields are written as

$$\dot{\mathbf{u}} = \mathbf{N}_u^s \dot{\bar{\mathbf{u}}}, \ \dot{p} = \mathbf{N}_p^s \dot{\bar{\mathrm{p}}}, \ \ddot{\mathbf{u}} = \mathbf{N}_u^s \ddot{\bar{\mathbf{u}}}, \ \ddot{p} = \mathbf{N}_p^s \ddot{\bar{\mathrm{p}}} \tag{22}$$

3.2 Outside fluid model

For the structures such as dam-reservoir systems, storage tanks or water containers we can assume that the contained fluid undergoes small motion which allow us to describe the fluid motion with Lagrangian formulation, and to derive governing equations from the acoustic wave theory. Here, we can assume that the fluid is incompressible, inviscid and homogeneous with the constant density. For finite element discretization of the fluid motion we choose mixed displacement/pressure based finite element formulation. The system of equations governing the discrete problem can be derived from variational formulation proposed in (Bathe *et al.* 1995, Wang and Bathe 1997), written as

$$\Pi = \int_{\Omega_f^e} \left[-\frac{p^2}{2\beta} - p(\nabla \cdot \mathbf{u}) - \frac{\boldsymbol{\Lambda} \cdot \boldsymbol{\Lambda}}{2\alpha} + \boldsymbol{\Lambda} \cdot (\nabla \times \mathbf{u}) - \mathbf{u} \cdot \mathbf{f}^b \right] d\Omega \tag{23}$$

where $\mathbf{u}$ is the displacement vector, p is the pressure, $\boldsymbol{\Lambda}$ is the 'vorticity moment', β is the bulk modulus of the outside fluid, α is the penalty parameter enforcing zero vorticity and $\mathbf{f}^b$ is the external load vector, which among body forces includes inertia force $-\rho\ddot{\mathbf{u}}$ as well.

By performing standard finite element procedure, and introducing finite element approximations in the weak form, obtained from the first variation of Eq. (23), we obtain following system of equations governing the discrete problem, written as

$$\begin{bmatrix} \mathbf{A}^{uu} & 0 & 0 \\ 0 & 0 & 0 \\ 0 & 0 & 0 \end{bmatrix}^e \begin{Bmatrix} \ddot{\bar{\mathbf{u}}} \\ \ddot{\bar{\mathbf{p}}} \\ \ddot{\bar{\boldsymbol{\lambda}}} \end{Bmatrix}^e + \begin{bmatrix} 0 & \mathbf{L}^{up} & \mathbf{L}^{u\lambda} \\ \mathbf{L}^{pu} & \mathbf{L}^{pp} & 0 \\ \mathbf{L}^{\lambda u} & 0 & \mathbf{L}^{\lambda\lambda} \end{bmatrix}^e \begin{Bmatrix} \bar{\mathbf{u}} \\ \bar{\mathbf{p}} \\ \bar{\boldsymbol{\lambda}} \end{Bmatrix}^e = \begin{Bmatrix} \mathbf{f}^f \\ 0 \\ 0 \end{Bmatrix}^e \tag{24}$$

where

$$\begin{aligned} &\mathbf{A}^{uu} = \int_{\Omega_f^e} \rho \mathbf{N}_u^{f,T} \mathbf{N}_u^f d\Omega \\ &\mathbf{L}^{up} = -\int_{\Omega_f^e} \mathbf{V}^T \mathbf{N}_p^f d\Omega, \qquad \mathbf{L}^{u\lambda} = \int_{\Omega_f^e} \mathbf{D}^T \mathbf{N}_\lambda^f d\Omega, \\ &\mathbf{L}^{pp} = -\int_{\Omega_f^e} \frac{1}{\beta} \mathbf{N}_p^{f,T} \mathbf{N}_p^f d\Omega, \qquad \mathbf{L}^{\lambda\lambda} = -\int_{\Omega_f^e} \frac{1}{\alpha} \mathbf{N}_\lambda^{f,T} \mathbf{N}_\lambda^f d\Omega, \end{aligned} \tag{25}$$

For a typical finite element, we have

$$\begin{aligned}
&\mathbf{u} = \mathbf{N}_u^f \bar{\mathbf{u}}, \quad p = \mathbf{N}_p^f \bar{\mathbf{p}}, \quad \boldsymbol{\Lambda} = \mathbf{N}_\lambda^f \bar{\boldsymbol{\lambda}} \\
&\ddot{\mathbf{u}} = \mathbf{N}_u^f \ddot{\bar{\mathbf{u}}}, \quad \ddot{p} = \mathbf{N}_p^f \ddot{\bar{\mathbf{p}}}, \quad \ddot{\boldsymbol{\Lambda}} = \mathbf{N}_\lambda^f \ddot{\bar{\boldsymbol{\lambda}}} \\
&\nabla \cdot \mathbf{u} = \left(\nabla \cdot \mathbf{N}_u^f\right) \bar{\mathbf{u}} = \mathbf{V} \bar{\mathbf{u}} \\
&\nabla \times \mathbf{u} = \left(\nabla \times \mathbf{N}_u^f\right) \bar{\mathbf{u}} = \mathbf{D} \bar{\mathbf{u}}
\end{aligned} \tag{26}$$

where $\mathbf{N}_u^f, \mathbf{N}_p^f, \mathbf{N}_\lambda^f$ are interpolation matrices, $\bar{\mathbf{u}}$ is the vector of unknown displacements, $\bar{\mathbf{p}}$ is the vector of unknown pressures, and $\bar{\boldsymbol{\lambda}}$ is the vector of unknown 'vorticity moments'.

The strong form of governing equations follows from (23), and can be written as

$$\nabla p + \nabla \times \boldsymbol{\Lambda} - \mathbf{f}^b = 0 \tag{27}$$

$$\nabla \cdot \mathbf{u} + \frac{p}{\beta} = 0 \tag{28}$$

$$\nabla \times \mathbf{u} - \frac{\boldsymbol{\Lambda}}{\alpha} = 0 \tag{29}$$

Here, for the discretization of the fluid domain we choose **Q4-P1-Λ1** finite elements (Fig. 5). These elements provide linear interpolation for the displacement fields, and constant approximations for the pressure and the 'vorticity moment'.

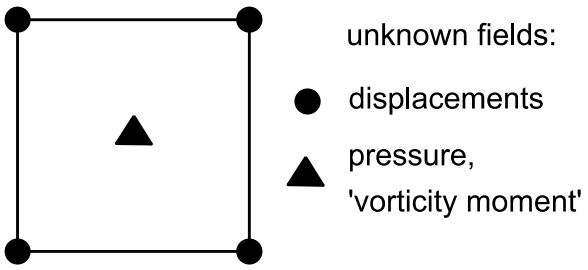

Fig. 5 Outside fluid finite element **Q4-P1-Λ1**

For solving global system of equations (Eq. (25)), we perform static condensation procedure where we statically condense the pressure and the 'vorticity moment' at the element level. The unknown values of the pressure and 'vorticity moment' are obtained from computed values of nodal displacements. In order to connect the fluid and structure finite elements at the fluid-structure interface we need to have a finite element that has both displacement and pressure degrees of freedom per node. To obtain **'Q4-P4'** type of finite element, we reconstruct the pressure field. Namely, we extrapolate the pressure computed inside each finite element to the nodes of **Q4** finite elements used for displacement approximations. The value of pressure at each node in the mesh of **Q4** finite elements is evaluated as an average value of the pressures computed in the finite elements that share that node.

4. Numerical results

In this section we present the results of numerical simulations which illustrate the capabilities of the proposed numerical model of acoustic fluid-structure interaction. First, we validate the numerical model of the pore-saturated structure and the outside fluid in dynamic setting, separately. Second, we observe a linear elastic separator wall with vertical upstream face subjected to horizontal ground acceleration. Here, we investigate and compare computed results against analytical solutions. Finally, we observe an inclined dam-reservoir system. All numerical computations are performed with a research version of the computer code FEAP, developed by R.L. Taylor (Zienkiewicz and Taylor 2005). In all numerical simulations, the meshing of the structure domain is carried out in GMSH using Delaunay triangulation (Geuzine and Remacle 2009).

4.1 Saturated poro-elastic column subjected to sinusoidal loading

In this example, we perform a validation computation of the proposed discrete model of saturated porous media in dynamic setting. We observe a saturated poro-elastic column subjected to sinusoidal loading (Fig. 6), defined with following expression

$$F = 3\left[1-\cos(\omega t)\right]\ \left[kN/m^2\right]; \quad \omega = 75\ s^{-1}$$

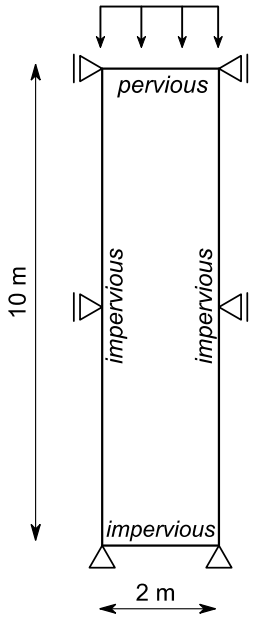

Fig. 6 Saturated poro-elastic column: Geometry and boundary conditions

We compare the computed results against the reference values provided in (De Boer *et al.* 1993), which are obtained with continuum model. The computation in continuum model in (de

Boer *et al.* 1993) is carried out for the values of Lame's parameters equal to $\lambda = 5.5833$ MPa and $\mu = 8.3750$ MPa, which correspond to Young's modulus and Poisson's ratio equal to $E = 20.10$ MPa and $v = 0.2$. The linear elastic parameters of the Timoshenko beam finite element are identified by exploiting the property that the linear elastic macro-scale response computed with discrete lattice model based on Voronoi cell representation of the domain matches the linear elastic response of an equivalent continuum model (Ibrahimbegovic and Delaplace 2003). Hence, the corresponding Young's modulus of Timoshenko beam finite element is $E = 23.71$ MPa, and the Poisson's ratio is selected as $v = 0$. The mass density of the porous medium is $\rho = 1670$ kg/m^3, and the coefficient of permeability is $k = 10^{-2}$ m/s.

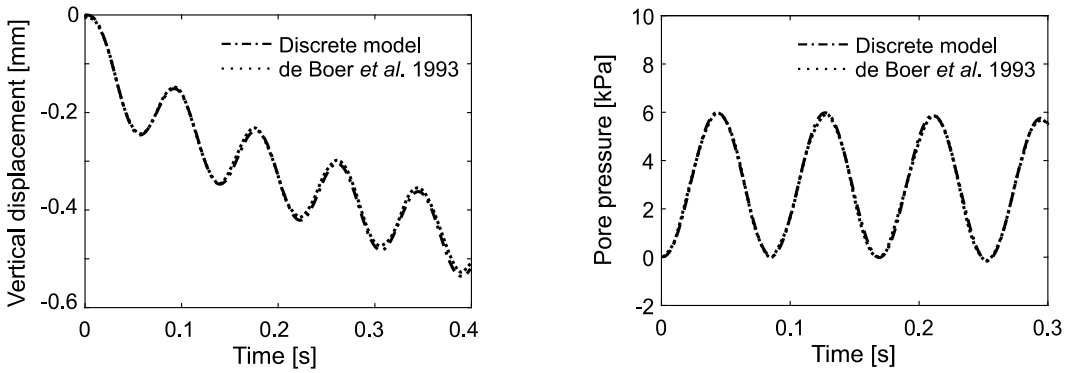

(a) Vertical displacement of column top (b) Pore pressure at $y = 6$ m

Fig. 7 Saturated poro-elastic column, computed results

The computed vertical displacement of the column top and the pore pressure at the depth $y = 6$ m (measured from the column top), shown in Fig. 7(a) and 7(b), show an excellent agreement with the reference values provided in (de Boer *et al.* 1993). We can conclude that the coefficient permeability of the coupled discrete beam lattice model matches the coefficient of permeability of an equivalent continuum model. Hence, it can be easily identified form standard experimental tests.

4.2 Modal analysis of rigid cavity problem

In this example, we perform the modal analysis of the rigid cavity problem in order to validate the proposed outside fluid model, which is based on **Q4-P1-Λ1** finite elements. The geometry and the boundary conditions of the problem are shown in Fig. 8. The density of the fluid is $\rho_f = 1000$ kg/m^3, the bulk modulus is $\beta = 115.6$ MPa, and the penalty parameter is $\alpha = 10^3\beta$. We compare the computed values of the first four frequencies against those provided in (Hamdi *et al.* 1978) and (Wang and Bathe 1997), which were computed from analytical frequency solution defined with following expression

$$\omega = c\pi\sqrt{\left(\frac{n}{a}\right)^2 + \left(\frac{m}{b}\right)^2} \tag{30}$$

where n, m are integers and c is the acoustic wave speed.

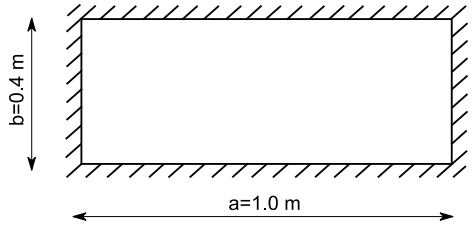

Fig. 8 Rigid cavity problem: Geometry and boundary conditions

The computed values of the first four frequencies are shown in Table 1. We can conclude that by increasing the mesh density, the results obtained with **Q4-P1-Λ1** finite elements approach the analytical solution.

Table 1 Rigid cavity problem: Computed frequencies

Mesh density	Frequency [Hz]			
4×3	174.4	374.9	444.6	463.0
8×6	171.1	348.8	429.9	459.3
32×24	170.1	340.5	425.3	457.8
64×48	170.0	340.1	425.1	457.8
Analytical solution	170.0	340.0	425.0	457.7

4.3 Linear elastic separator wall

In this example we present the results of the first numerical simulation of acoustic fluid-structure interaction. We observe a linear elastic separator wall 12 m high, and 1.2 m thick. The configuration of the problem is shown in Fig. 9. The Young's modulus of the wall is $E=10^4$ MPa, the Poisson's ratio is $\nu=0.3$, the mass density is $\rho_s=2000$ kg/m^3, and the coefficient of permeability is $k=10^{-6}$ m/s. The mass density of the outside fluid is $\rho_f=1000$ kg/m^3 and the bulk modulus is $\beta=10^5$ MPa.

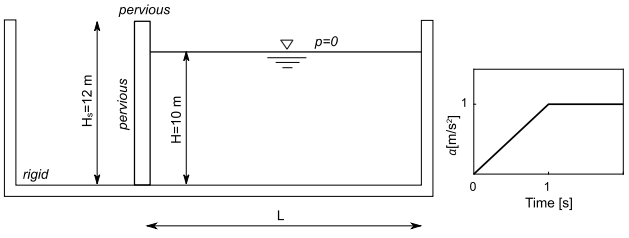

Fig. 9 Linear elastic separator wall: Geometry, boundary conditions and loading program

We subject the separator wall and the contained fluid to a horizontal ground acceleration reaching its maximum value of $a_0 = 0.1$ g at $t = 1$ s, after which is kept constant (Fig. 9). According to (Chopra 2012), we model the horizontal ground movement in terms of equivalent horizontal forces acting on the system with fixed base. We compare the computed values of hydrodynamic pressure exerted on the wall against those provided in (Chwang 1978) with the aim to validate the proposed model for predicting hydrodynamic pressures and hydrodynamic forces exerted on the upstream face of the structure.

We present the results in terms of the pressure coefficient C_p. We compare the computed results against reference values provided by (Chwang 1978). Computed values of pressure coefficient for different values of L/H ratio are shown in Fig. 10(a). We can conclude that the values of hydrodynamic pressure depend on the length of the outside fluid domain, because of the influence of boundary effects at the infinity. For values of L/H ratio greater than 3, results do not differ significantly and approach the analytical solution.

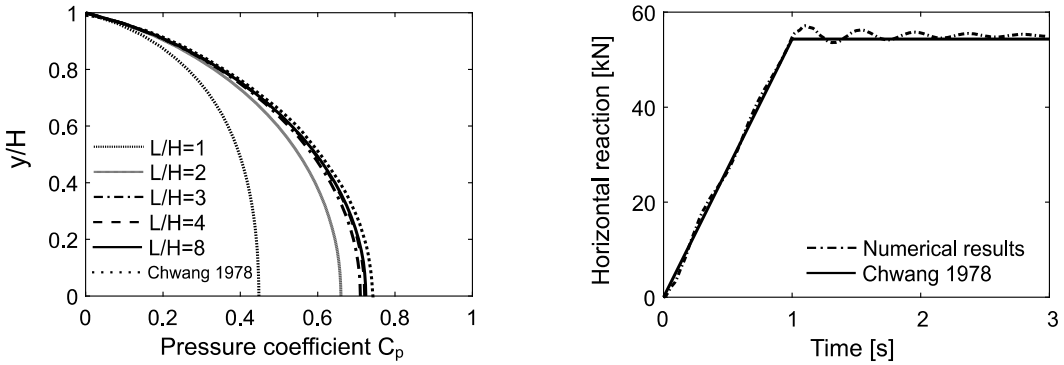

(a) C_p for different L/H ratio (b) Horizontal force for $L/H = 8$

Fig. 10 Linear elastic separator wall, computed results

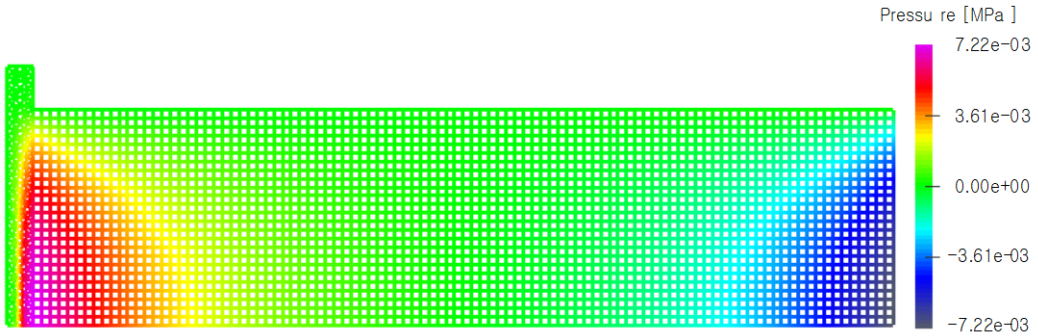

Fig. 11 Pressure and pore pressure distribution, $L/H = 4$

We also investigate the influence of the fluid acting as a source of additional forces on the structure. The reference value of total horizontal force exerted on the vertical upstream face of the structure is given in (Chwang 1978). We compare this reference value against the computed value of horizontal force exerted on the upstream face of the separator wall. The value of horizontal

force is computed on a numerical model of acoustic fluid-structure interaction, in which only the reservoir was subjected to horizontal ground acceleration. The results are shown in Fig. 10(b). We can conclude that as the oscillations of the separator wall are being damped, the computed results approach the reference value. This confirms that with the proposed model we are able to ensure the direct transfer of both forces and pressures at the fluid-structure interface. It should be noted that no artificial damping (e.g., Rayleigh damping) is added in the numerical model of the fluid-structure interaction. The damping in the numerical model results solely from the equations governing the coupled problem. The hydrodynamic pressure distribution in the fluid domain, and pore pressure distribution in the separator wall for $L/H=4$ are shown in Fig. 11.

4.4 Inclined dam-reservoir system

In this example, we observe a dam-reservoir system. The geometry and boundary conditions are shown in Fig. 12. The faces of the dam are inclined with a constant angle of $\theta=45°$. The height of the fluid in the reservoir is $H=7.9$ m, and the length of the reservoir is $L=60$ m. The length of the reservoir is chosen so that the influence of boundary effects on the computed results is eliminated. The mechanical properties of the dam are: Young's modulus $E=50$ MPa, Poisson's ratio $v=0.3$, the mass density $\rho_s=2000$ kg/m^3, and the coefficient of permeability $k=10^{-5}$ m/s. The mechanical properties of the outside fluid are: the mass density $\rho_f=1000$ kg/m^3, and the bulk modulus $\beta=1000$ MPa. The loading program consists of two phases. We first apply hydrostatic loading. Next, we subject the dam-reservoir system to horizontal ground acceleration $a_0=0.1$ g. We compare the computed results against analytical solution provided by (Chwang 1978).

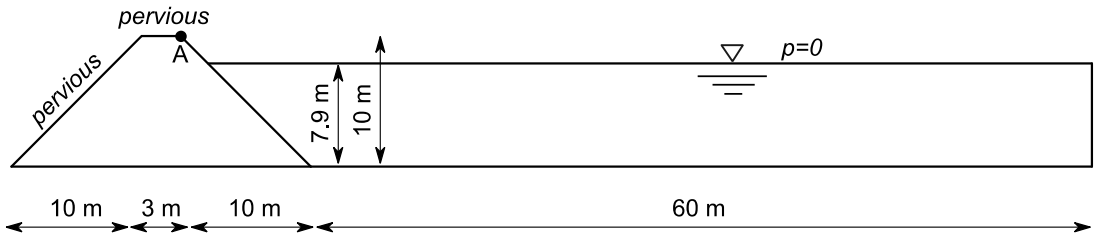

Fig. 12 Inclined dam-reservoir system: Geometry and boundary conditions

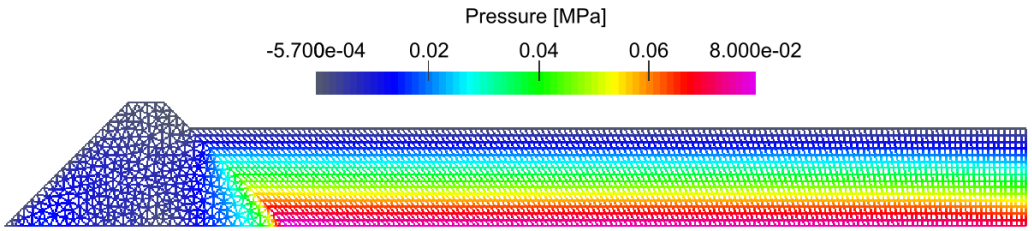

Fig. 13 Pressure and pore pressure distribution in inclined dam-reservoir system

The distribution of pressures in the fluid domain, and the pore pressures in the body of the dam are shown in Fig. 13. The comparison of the computed values of hydrodynamic pressure and the analytical solution are shown in Fig. 14. We can conclude that a good match between the

compared values is obtained. With the proposed numerical model of acoustic fluid-structure interaction, we are able to predict the hydrodynamic pressure distribution on the upstream face of the dam and also to trace the values of the pore pressure in the body of the dam at each time step. This is very important in the case of earth dams, where an increase in pore pressures in dynamic setting can lead to the liquefaction where soil completely loses its strength and begins to flow like a fluid.

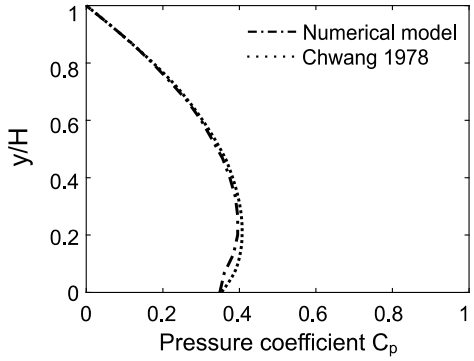

Fig. 14 Dam-reservoir system: comparison of computed and reference values of pressure coefficient C_p

The outside fluid acts also as a source of additional forces on the structure. The total horizontal and vertical reaction at the bottom of the dam are shown in Fig. 15(a) and 15(b). We can conclude that the proposed model ensures the direct transfer of both the forces and pressures, without any special numerical treatment of the fluid-structure interface.

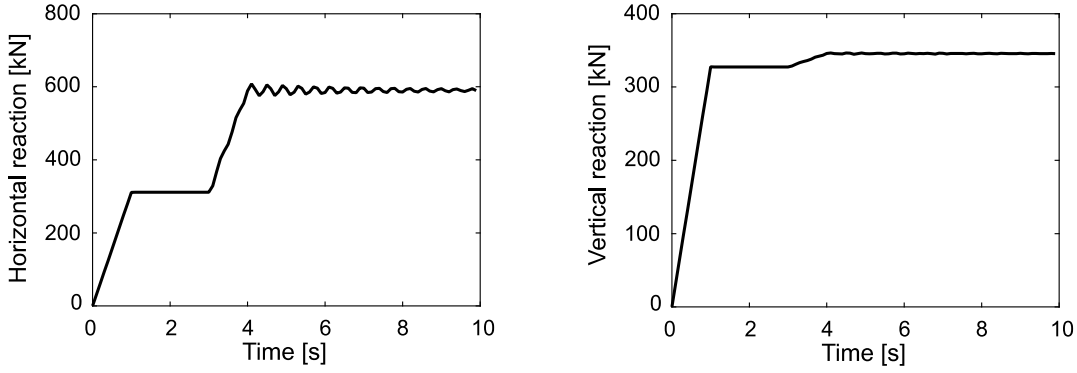

(a) Horizontal reaction (b) Vertical reaction

Fig. 15 Dam-reservoir system, computed results

To validate our results, we compare the computed value of the horizontal force exerted on the upstream face of the dam that results from the outside fluid acting as a source of the loading, against the analytical value of the horizontal force exerted on the inclined dam (Fig. 16(a)). The

value of horizontal force is computed in the same manner as for the case of separator wall, by only subjecting the outside fluid to horizontal ground acceleration. The computation is performed without first subjecting the dam-reservoir system to hydrostatic loading phase. We can conclude that a good match between the computed and reference values is obtained. The horizontal displacements of the tip of the dam (point *A*) are shown in Fig. 16(b).

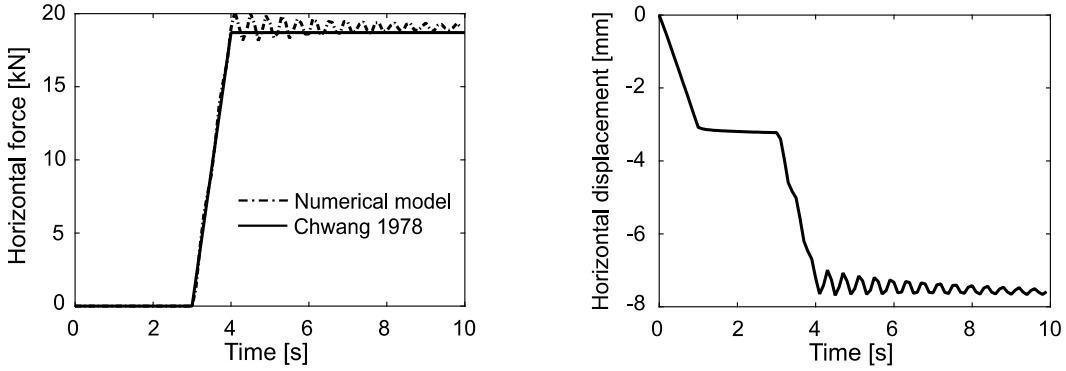

(a) Horizontal force (b) Horizontal displacement at point *A*

Fig. 16 Dam-reservoir system, computed results

With the proposed numerical model of acoustic fluid-structure interaction, in which the structure response is obtained on the mesh of one-dimensional Timoshenko beam finite elements, it becomes relatively simple to implement any other constitutive model that is capable of reproducing different kind of phenomena observed in structures. Here, we provide an illustrative example of one such model. Namely, we assume that the response of the Timoshenko beam finite element is governed by plasticity with linear isotropic hardening (Ibrahimbegovic 2009). We introduce yield limits in tension, compression and shear are: $\sigma_{y,t}=0.01$ MPa, $\sigma_{y,c}=0.1$ MPa, and $\sigma_{y,s}=0.01$ MPa. The computed horizontal displacements at point *A* are shown in Fig. 17. The plastic zones formed in the body of the dam are shown in Fig. 18(a) and 18(b).

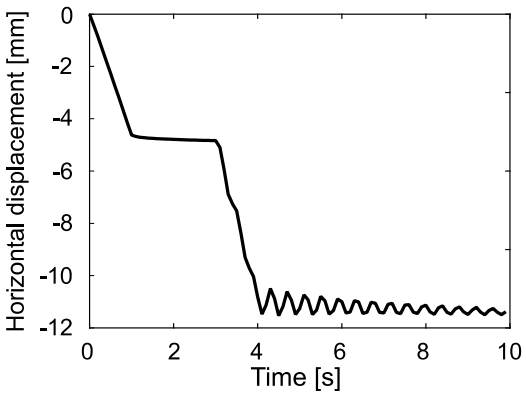

Fig. 17 Nonlinear dam-reservoir system, computed results: Horizontal displacement at point *A*

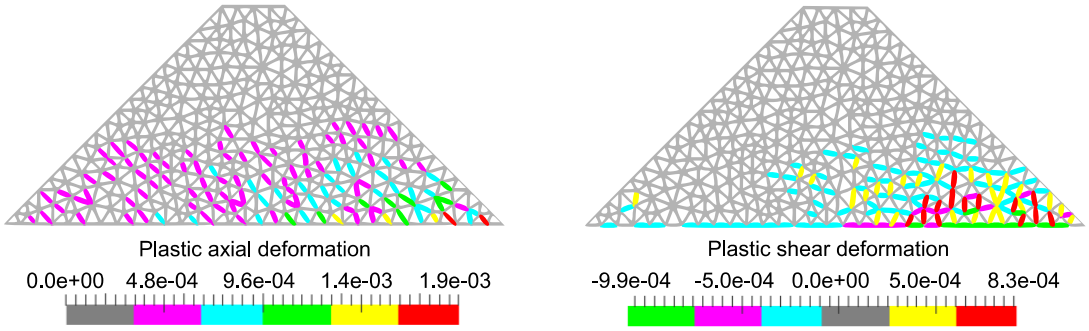

(a) Plastic axial deformation (b) Plastic shear deformation

Fig. 18 Nonlinear dam-reservoir system, computed results: Plastic zones

5. Conclusions

In this paper, we presented a numerical model of acoustic fluid-structure interaction in dynamic setting. In the proposed model, the structure is modeled as a saturated porous medium whose response is obtained with coupled discrete beam lattice model based on Voronoi cell representation with cohesive links as linear elastic Timoshenko beam finite elements. The motion of the outside fluid is described with mixed displacement/pressure based formulation.

Based on the results presented in this paper, we can conclude that the proposed numerical model is able to predict the values and the distribution of the hydrodynamic pressure for the general case of an inclined upstream face of the structure in close agreement with analytical solutions, and also to predict the total values of the horizontal and vertical force exerted on the structure subjected to combined static and dynamic loading. The main strength of the proposed model is that the outside fluid and structure finite elements share both the displacement and pressure degrees of freedom which eliminates any need for special numerical considerations of the fluid-structure interface. The proposed model is predictive and simple enough, and thus can be used as an everyday tool in structural analysis.

The proposed model could also serve as a powerful tool for analyzing the liquefaction phenomena in earth dams, since we are able to track the pore pressure evolution in the body of the dam throughout the loading program. Here, any other constitutive model that is able to reproduce the failure modes for different materials can be easily implemented because of the use of one-dimensional finite elements in the numerical model of the structure.

Acknowledgments

This work was supported by the French Ministry of Foreign Affairs, and French Embassy in Bosnia and Herzegovina. Professor Adnan Ibrahimbegovic was supported by the funding for Chaire de Mécanique Picardie (120-2015 RDISTRUCT-000010 and RDISTRUCT-000010) with EU funding (FEDER) and IUF-Institut Universitaire de France (Membre Senior). These grants and financial supports are gratefully acknowledged.

References

Bathe, K.J., Nitikitpaiboon, C. and Wang, X. (1995), "A mixed displacement-based finite element formulation for acoustic fluid-structure interaction", *Comput. Struct.*, **56**(2-3), 225-237.

Benkemoun, N., Hautefeuille, M., Colliat, J.B. and Ibrahimbegovic, A. (2012), "Failure of heterogeneous materials: 3D meso-scale FE models with embedded discontinuities", *Int. J. Numer. Meth. Eng.*, **82**, 1671-1688.

Benkemoun, N., Ibrahimbegovic, A. and Colliat, J.B. (2012), "Anisotropic constitutive model of plasticity capable of accounting for details of meso-structure of two-phase composite material", *Comput. Struct.*, **90**, 153-162.

Biot, M.A. (1941), "General theory of three-dimensional consolidation", *J. Appl. Phys.*, **12**(2), 155-164.

Chen, H.C. and Taylor, R.T. (1990), "Vibration analysis of fluid-solid systems using a finite element displacement formulation", *Int. J. Numer. Meth. Eng.*, **29**(4), 683-698.

Chopra, A.K. (2012), *Dynamics of Structures: Theory and Applications to Earthquake Engineering*, Prentice Hall.

Chwang, A.T. (1978), "Hydrodynamic pressures on sloping dams during earthquakes. Part 2. Exact theory", *J. Flu. Mech.*, **87**(2), 343-348.

Chwang, A.T. and Housner, G.W. (1978), "Hydrodynamic pressures on sloping dams during earthquakes. Part 1. Momentum method", *J. Flu. Mech.*, **87**(2), 335-341.

De Boer, R., Ehlers, W. and Liu, Z. (1993), "One-dimensional transient wave propagation in fluid-saturated incompressible porous media", *Arch. Appl. Mech.*, **63**(1), 59-72.

Geuzaine, C. and Remacle, J.F. (2009), "Gmsh: A 3-D finite element mesh generator with built-in pre- and post-processing facilities", *Int. J. Numer. Meth. Eng.*, **79**, 1309-1331.

Hadzalic, E., Ibrahimbegovic, A. and Dolarevic, S. (2018), "Failure mechanisms in coupled soil-foundation systems", *Coupled Syst. Mech.*, **1**, 27-42.

Hadzalic, E., Ibrahimbegovic, A. and Nikolic, M. (2018), "Failure mechanisms in coupled poroplastic medium", *Coupled Syst. Mech.*, **1**, 43-59.

Hamdi, M.A., Ousset, Y. and Verchery, G. (1978), "A displacement method for the analysis of vibrations of coupled fluid-structure systems", *Int. J. Numer. Meth. Eng.*, **13**(1), 139-150.

Ibrahimbegovic, A. (2009), *Nonlinear Solid Mechanics: Theoretical Formulations and Finite Element Solution Methods*, Springer.

Ibrahimbegovic, A. and Delaplace, A. (2003), "Microscale and mesoscale discrete models for dynamic fracture of structures built of brittle material", *Comput. Struct.*, **81**, 1255-1265.

Keivani, A., Shooshtar, A. and Sani, A.A. (2013), "A closed form solution for a fluid-structure system: Shear beam-compressible fluid", *Coupled Syst. Mech.*, **2**(2), 127-146.

Mandal, K.K. and Maity, D. (2015), "2d finite element analysis of rectangular water tank with separator wall using direct coupling", *Coupled Syst. Mech.*, **4**(4), 317-336.

Matsuzawa, H., Ishibashi, I. and Kawamura, M. (1985), "Dynamic soil and water pressures of submerged soils", *J. Geotech. Eng.*, **111**(10), 1161-1176.

Mitra, S. and Sinhamahapatra, K.P. (2008), "2d simulation of fluid-structure interaction using finite element method", *Fin. Elem. Analy. Des.*, **45**(1), 52-59.

Nikolic, M. and Ibrahimbegovic, A. (2015), "Rock mechanics model capable of representing initial heterogeneities and full set of 3D failure mechanisms", *Comput. Meth. Appl. Mech. Eng.*, **290**, 209-227.

Nikolic, M., Ibrahimbegovic, A. and Miscevic, P. (2015), "Brittle and ductile failure of rocks: Embedded discontinuity approach for representing mode I and mode II failure mechanisms", *Int. J. Numer. Meth. Eng.*, **102**, 1507-1526.

Nikolic, M., Ibrahimbegovic, A. and Miscevic, P. (2016), "Discrete element model for the analysis of fluid-saturated fractured poro-plastic medium based on sharp crack representation with embedded strong discontinuities", *Comput. Meth. Appl. Mech. Eng.*, **298**, 407-427.

Pelecanos, L., Kontoe, S. and Zdravkovic, L. (2013), "Numerical modelling of hydrodynamic pressures on

dams", *Comput. Geotech.*, **53**, 68-82.
Von Kármán, T. (1933), "Discussion of water pressures on dams during earthquakes", *Trans. ASCE*, **98**, 434-436.
Wang, X. and Bathe, K.J. (1997), "Displacement/pressure based mixed finite element formulations for acoustic fluid structure interaction problems", *Int. J. Numer. Meth. Eng.*, **40**(11), 2001-2017.
Wang, X. and Wang, L.B. (2007), "Dynamic analysis of a water-soil-pore water coupling system", *Comput. Struct.*, **85**(11), 1020-1031.
Westergaard, H.M. (1933), "Water pressures on dams during earthquakes", *Trans. ASCE*, **98**, 418-432.
Zienkiewicz, O.C. and Bettess, P. (1978), "Fluid-structure dynamic interaction and wave forces. An introduction to numerical treatment", *Int. J. Numer. Meth. Eng.*, **13**(1), 1-16.
Zienkiewicz, O.C. and Taylor, R.L. (2005), *The Finite Element Method, Vols. I, II, III*, Elsevier.

AI